Available online at www.sciencedirect.com
ScienceDirect
Ceramics International 37 (2011) 451–464
CERAMICS INTERNATIONAL
www.elsevier.com/locate/ceramint

Morphological studies of randomized dispersion magnetite nanoclusters coated with silica

C.Y. Haw [a], C.H. Chia [a,*], S. Zakaria [a], F. Mohamed [a], S. Radiman [a], C.H. Teh [b], P.S. Khiew [c], W.S. Chiu [d], N.M. Huang [d]

[a] School of Applied Physics, Faculty of Science and Technology, Universiti Kebangsaan Malaysia, 43600 Bangi, Selangor, Malaysia
[b] School of Chemical Sciences and Food Technology, Faculty of Science and Technology, Universiti Kebangsaan Malaysia, 43600 Bangi, Selangor, Malaysia
[c] Faculty of Engineering, University of Nottingham Malaysia Campus, Jalan Broga, 43500 Semenyih, Selangor, Malaysia
[d] Solid State Physics Research Laboratory, Physics Department, University of Malaya, 50603 Kuala Lumpur, Malaysia

Received 9 July 2010; received in revised form 6 August 2010; accepted 2 September 2010
Available online 25 September 2010

Abstract

In this study, we report a simple way to produce randomized dispersion magnetite nanoclusters coated with silica (RDMNS) via Stöber process with minor modifications. The morphology of silica coated magnetite nanoclusters was emphasized by studying various reaction parameters including alcohols with different polarities as co-solvents, concentration of alcohol–water, concentration of alkaline catalyst (ammonia), and concentration of TEOS monomer. The results of transmission electron microscope (TEM) showed that the sizes and morphological behaviour of the magnetite nanoclusters vary accordingly with the different reaction parameters investigated. The results showed that ethanol would be the best candidate as co-solvent in the preparation of randomized dispersion magnetite nanoclusters. Besides, the optimum alcohol–water ratio has been determined to be 70–30% v/v as this concentration range could render desired shape of randomized dispersion magnetite nanoclusters. The volume of ammonia (NH_3) catalyst in the reaction media also strongly governs the formation of silica coated magnetite nanoclusters in a desired shape. Apart from that, the addition of TEOS monomer into the reaction media has to be well-controlled as the excess amount of monomer added might affect the thickness of the silica layer that is coated on the magnetite nanoparticles. Prior to silica coating, the bare magnetite nanoparticles were first treated with trisodium citrate (0.5 M) to enhance the particles' dispersibility. Improvement in the size distribution and dispersibility of the magnetite nanoparticles after the citrate treatment has been examined using TEM. The XRD results show that the magnetite samples retained good crystallinity although they have been surface-modified with citrate group and silica. The Fourier transform infrared (FT-IR) and thermogravimetric analysis (TGA) prove that the magnetite nanoparticles have been successfully coated with citrate and silica. The superparamagnetic behaviour of the magnetite samples was confirmed by VSM. The produced silica coated magnetite nanoclusters possess great potential to be applied in biomedical research and clinical diagnosis application.

Keywords: B. Surfaces; C. Magnetic properties; E. Biomedical applications; Magnetic nanoclusters

1. Introduction

Nanofabricated magnetite nanoparticles have been an intense focus of fundamental researchers since last decade because they have unique magnetic properties and ease to be engineered into many forms of composite materials, typically for biomedical applications. There are a number of synthetic methods being utilized to produce nanoscaled magnetite particles like, organo-metallic thermal decomposition [1], microemulsion [2], hydrothermal [3], solvothermal [4], and co-precipitation [5,6]. The latter is the most commonly used method, mainly attributed to its simple and easy processing operation, high yield of products with superior crystallinity and magnetic behaviours and it involves only the utilization of non-organic based reactants. However, the major shortcoming of this method is the agglomeration of the particles due to their high magnetization properties.

To date, several findings have shown that the nanoparticles are favorably synthesized in the form of nanoclusters [7,8]. Magnetic nanoclusters are a type of magnetic nanoscale

* Corresponding author. Tel.: +60 3 89215473; fax: +60 3 89213777.
E-mail address: chia@ukm.my (C.H. Chia).

0272-8842/$36.00
doi:10.1016/j.ceramint.2010.09.010

materials containing a number of magnetic nanoparticles embedded or enwrapped by a polymeric shell such as thermoresponsive polymers [9], cyclodextrin [10], chitosan [11], and carbon nanocomposites [12]. These magnetic nanoclusters can easily be magnetized by an external magnetic field and loss of signal will greatly be avoided when it is in vivo transported together with the drugs to the targeted site. Previous studies have reported that the magnetic nanoparticles will tend to lose the magnetizability when the biopolymer coated nanoparticles are being carried into the body [13]. In the targeting drug delivery system, sufficient amount of drug is needed to be carried to the targeted organ by incorporating it with surface-functionalized magnetic nanoclusters under the manipulation of external magnetic field [14]. However, usually the nanoparticles coated insufficiently will have the difficulty to be magnetized by external magnetic field, resulting in lower efficiency of drug targeting treatment and to some extent the drug being transported may be erupted from the polymeric shell causing local cytotoxicity. Therefore, attention needs to be drawn towards the study of nanocluster formation due to their intriguing physical and chemical properties. However, formation of magnetic nanoclusters is a grand challenge bound to the magnetic properties of the particles, type of surface modifier whether it is dispersible in organic or non-organic solvent, biocompatibility of modifier and reproducibility. Therefore, particle dispersity is an issue that needs to be addressed earnestly in order to overcome the agglomeration of magnetic nanoparticles before the formation of magnetic nanoclusters. As a result, in this study, we adopted polyanionic citrate group to improve the dispersibility of the magnetite nanoparticles so that the nanoparticles can be homogeneously coated with the silica material. Previous study reported that the addition of anionic citrate to the surface of magnetite nanoparticles through chemical complexation process has greatly improved the particle's dispersibility [15].

Essentially, there are four types of nanocluster morphology including core–shell structure, reverse core–shell, interlayered, and randomized dispersions [16–19]. In this study, we are interested in the randomized dispersion nanoclusters since this particular morphology of nanoclusters offers larger cavity for the embedded seeds to be covered by the polymer layer. Fig. 1 depicts the typical type of nanoclusters in which the nanoseeds are randomly dispersed in the protective cavity resulting from the coating process.

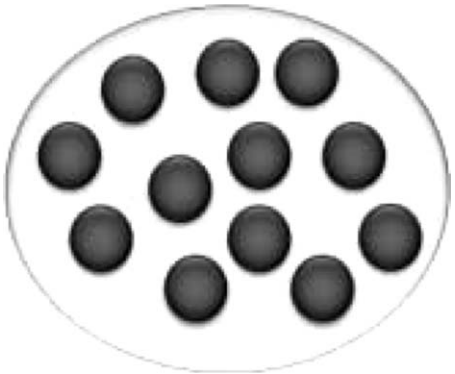

Fig. 1. Randomized dispersion nanoclusters.

Although many investigations have been done on the silica coated magnetite nanoparticles, however, to the best of our knowledge, the study of magnetic nanocluster formation has not been well developed. Silica is well-known for its biocompatibility, microporous properties, and excellent reproducibility [20–22]. However, most of the studies reported irregular shape of silica coating and showed severe agglomeration of the magnetic coated silica instead of well-confined in a silica shell [21,23]. To have better understanding on the effect of silica coating on the magnetic nanoparticle surfaces, pretreatment of magnetic nanoparticle surfaces is necessary in order to overcome the agglomeration of particles. Another issue that needs to be ascertained is the essential processing parameters that need to be adapted during the formation of silica material, in order to enhance the efficiency in the production of mono-dispersed silica spheres. Chou and Chen studied the critical condition related to the formation of new secondary silica particles during the seeded nucleation process [24]. They had varied the amount of TEOS to tune the size and shape of the amorphous silica particles.

In the present study, we have synthesized randomized dispersion magnetite nanoclusters using silica with minor modification from Stöber process. We have studied different reaction parameters including the different polarities of alcohol, ratio of alcohol–water as co-solvent, concentration of ammonia as catalyst, and concentration of TEOS monomer. The as-synthesized magnetite nanoparticles, citrate-treated magnetite nanoparticles, and RDMNS were then characterized using various instrumentations including morphology and size determination by transmission electron microscopy (TEM), degree of crystallinity before and after surface modification by X-ray diffraction (XRD), retainability of superparamagnetic properties of citrate and silica modified magnetite nanoparticles by vibrating sample magnetometer (VSM), the presence of citrate and silica layers on the surface of magnetite nanoparticles by Fourier transform infra red spectroscopy (FT-IR) and percentage of citrate and silica coated on the magnetite nanoparticles using thermogravimetric analysis (TGA). The mechanism of citrate-attachment to the magnetite nanoparticles surface will also be discussed.

2. Experimental

2.1. Materials

Chemicals were used as received without further purification. Analytical-grade TEOS (tetraethyl orthosilicate, ≥98%), ethyl alcohol (>99%), NH_3 (ammonia solution, 28 wt.%), and NaOH pellets (sodium hydroxide, assay ≥97%) were purchased from Merck & Co., Inc.; whilst ferrous dichloride heptahydrate ($FeCl_2{\cdot}4H_2O$), ferric trichloride anhydrous $FeCl_3$, trisodium citrate dihydrate (assay 99.3%), and methanol (ACS reagent, ≥99.8%) were procured from Sigma–Aldrich. Deionized water (DIW) was used throughout the experiment and degassed for 30 min prior to the experiments. All experiments were carried out at room temperature (25 ± 1 °C).

2.2. Methods

2.2.1. Preparation of magnetite nanoparticles

Magnetite nanoparticles were prepared using co-precipitation method [5,7]. Briefly, 0.02 mol of $FeCl_2{\cdot}4H_2O$ (6.48 g) and 0.04 mol of $FeCl_3$ anhydrous (3.97 g) were dissolved in 150 ml of deoxygenated water. The above mixture was kept in constant stirring under ambient temperature before being transferred into a three necked flask of 250 ml cavity. In this regard, argon gas was constantly supplied into the ferrous and ferric mixture to expel the dissolved oxygen in the solution. On the other hand, NaOH (about 10 M) solution was also prepared and added into the reaction mixture after constant stirring for 30 min. A black suspension could be observed immediately upon the addition of NaOH solution into the reaction mixture. The pH of the suspension was found to be around 10–11 with the aid of pH meter. Afterwards, the temperature of the suspension was slowly elevated to 80 °C for 1 h under mild stirring with argon gas purging to avoid rapid growth of nanoparticles. Subsequently, the resultant black suspension was cooled to room temperature and magnetically recovered. Then, the product was washed alternatively with DIW and ethyl alcohol for several times. Some of the obtained product was freeze-dried and the left over was redispersed into ethanol solution (80% v/v) for further treatment. The product obtained was denoted as M1.

2.2.2. Citrate modified magnetite nanoparticles

A replication of the above experiment was carried out. In this particular step, the introduction of citrate group onto the surface of magnetite nanoparticles was aimed to improve the dispersibility of the nanoparticles. Typically, 0.5 M of sodium citrate solution was prepared alongside with the procedure as stated in Section 2.2.1. As the black suspension of particles was obtained, the as-prepared 0.5 M of sodium citrate solution (35 ml) was added into the cooled black suspension and subsequently heated to 80 °C for 1 h. The modified nanoparticles were then cooled to room temperature and magnetically collected. The particles were then washed with DIW and ethyl alcohol to eliminate the unreacted compounds. Portion of the particles were redispersed in the same concentration (0.5 M) of citrate solution for further work. For instrumental analysis purposes, the left over particles were freeze-dried into powder form and the resulting product was defined as CM1.

2.2.3. Preparation magnetite nanoclusters coated with silica

Adopted from Stöber process [25], silica coated magnetite nanoclusters were synthesized with some modifications. In this section, a series of experiments with different parameters were performed to produce silica coated magnetite nanoclusters. Precursor TEOS was used for seed-mediated growth of silica on the surface of magnetite nanoparticles coated with citrate. Firstly, 2 ml of CM1 dispersion (containing about 880 mg) of magnetite nanoparticles was well mixed with alcohol (solvent), water, and ammonia (catalyst) solutions. The dispersion was later homogenized with ultrasonicator (70% of 200 W) in an icy bath. It should be noted that the interval of sonication must be as short as possible (set to 2 min pulse-on and 1 min pulse-off). This is because continuous high power sonication will produce large amount of heat which will induce transformation of magnetite phase into other unwanted iron oxide phases. During the pulse-on mode, the precursor TEOS was carefully dropped into the reaction mixture with the aid of syringe (3 ml). The homogenization was performed for 10 min. After sonication, the reaction mixture was immediately transferred into an Erlenmeyer flask (250 ml) and mechanically stirred overnight. The recipe of different chemicals for silica coating process is outlined in Table 1. Different parameters were elucidated to study their effect in producing randomized dispersion magnetite nanoclusters coated with silica. We were first examining the different polarities of alcohol that is essential in determining the size distribution and morphology of the nanoclusters. Haddad et al. had reported that the volume ratio of solvent–water plays an important role in determining the shape of silica-coated magnetite nanoparticles [26]. They found that low water volume will prevent rapid hydrolysis and condensation of TEOS. Therefore, in this study we only use low water volume i.e., 30 ml out of total volume of alcohol–water (100 ml). Followed with the type of solvent is chosen, we have studied the effect of different volumes of ammonia which

Table 1
Reaction parameters to produce silica coated magnetite nanoclusters.

Sample code	Alcohol	TEOS (ml)	Alcohol–water (% v/v)	NH_3 (28% v/v) (ml)
SCM1	Methanol	2	70	2
SCM2	Ethanol	2	70	2
SCM3	Isopropyl alcohol	2	70	2
SCM4	Tertiary alcohol	2	70	2
SCM-a	Ethanol	2	100	2
SCM-b	Ethanol	2	50	2
SCM-c	Ethanol	2	30	2
SCM-d	Ethanol	2	0	2
SCM-Am0.5	Ethanol	2	70	0.5
SCM-Am1	Ethanol	2	70	1
SCM-Am3	Ethanol	2	70	3
SCM-T3	Ethanol	3	70	2
SCM-T4	Ethanol	4	70	2

served as a catalyst in the formation of randomized dispersion magnetite nanoclusters. Finally, we have also determined the thickness of silica coating by varying the amount of TEOS added into the reaction mixture. The determined reaction parameter of silica coated magnetite nanoclusters is labelled as SCM.

2.2.4. Characterizations

2.2.4.1. TEM. The size distribution, morphology and shape of the as-synthesized nanoparticles for M1, CM1, and SCM samples were analyzed using a transmission electron microscope (Philips, CM-12) operated at 100 kV. Prior to the test, each sample was ultrasonicated for 10 min, then dropped gently onto the carbon coated Cu-grid aided with micropipette and left to dry at room temperature.

2.2.4.2. XRD. Powder X-ray diffraction spectra for the as-prepared samples were obtained using a Bruker D8 advance X-ray diffractometer operated at 40 kV and 40 mA with Ni-filtered Cu $K_{\alpha 1}$ radiation (1.5406 Å). The detector Sol-XE was used to inspect the crystallinity of M1, CM1, and SCM with which the latter one was prepared based on the pre-determined parameters of silica coated magnetite nanoclusters. Measurement of angle 2θ was set from 3° to 80° with increment of 0.025° per step of sample irradiation. For the sample preparation, silica crystal low background sample holders were employed to keep the powdery samples on the flat surface to optimise the sample irradiation as well as to keep the detection more efficient. Fig. 2 depicts a sample holder with the prescribed amount covered on the holder surface. After the test, the spectra were compared with the standard characteristic peaks provided by JCDPS 00-019-0629 of International Center for Diffraction Data.

2.2.4.3. FT-IR. Fourier-transform infrared examination was conducted to determine the presence of silica layer on the surface of the magnetite nanoclusters using a FTIR Perkin Elmer GX spectrophotometer in the range of 370–4000 cm^{-1}. The spectra were recorded at room temperature using KBr pellets. After the three batches of samples were inspected, the obtained spectra were plotted on the same graph. This can be qualitatively useful to distinguish the different functional groups that appeared on the pristine magnetite nanoparticles, citrate modified magnetite nanoparticles and SCM.

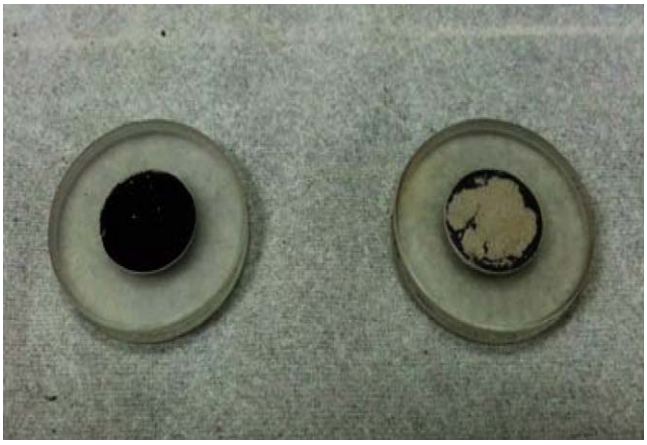

Fig. 2. Two silica crystal low background sample holders containing pristine magnetite nanoparticles (left) and powdery silica coated magnetite nanoparticles (right).

2.2.4.4. VSM. A vibrating-sample magnetometer (VSM, LakeShore 736) was used to measure the hysteresis loop and other important magnetic properties of the synthesized magnetic samples (M1, CM1, and SCM) at 298 K. Samples were placed in a special sample vial and vibrated at high speed to shear the applied magnetic field at the central position. The magnetic signal generated from the samples was picked up by the Gauss meter and hysteresis loops were obtained. Data were later processed and the magnetic information was analyzed and compared for different samples to determine their magnetic behaviour.

2.2.4.5. TGA. A Mettler Toledo TG analyzer was employed to perform the thermogravimetric analysis in order to further confirm the presence of citrate group and amorphous on the magnetic surface upon heating the three samples M1, CM1 and SCM. The heating rate was set to 10 °C/min in a thermobalance instrument. Typically, a thermal heating plate containing the samples was heated in a furnace at a controlled rate and weighed continuously on a balance. Temperature and mass data were collected and processed by a computer dedicated to the system. Any physical or chemical change in the samples could be elucidated analytically.

3. Results and discussion

3.1. Morphology and size distribution of M1 and CM1

Fig. 3 shows typical TEM micrographs of both the unmodified magnetite nanoparticles (M1) produced via concentrated precipitation method (10 M of NaOH) and the citrate-modified magnetite nanoparticles (CM1). Referring to Fig. 3 (A), majority of the particles were in oval shape and some least number of cubic shaped magnetite nanoparticles also can be observed. The average crystallite size for the M1 nanoparticles is about 9.14 ± 3.14 nm. On the contrary, CM1 nanoparticles which are of better dispersibility as shown in Fig. 3 (B) having an average particle size of 9.04 ± 4.33 nm. One can see that there was no significant change in the size or the morphology alterations of the M1 nanoparticles and CM1 nanoparticles. The modified nanoparticle size is in the range from 2.3 nm to 14.67 nm whilst the unmodified one is in the range between 4.5 nm and 17.8 nm. It is noteworthy that the citrate modified magnetite nanoparticles show narrower particles size distribution as compared to the unmodified nanoparticles. The discrepancy between the particles size distribution of both experiments might be explained by the physical and chemical properties of the particles themselves. Generally, magnetite nanoparticles that are synthesized by co-precipitation method normally will have a common undesired feature, i.e., the nanoparticles tend to agglomerate with the neighboring particles, as can be noted in Fig. 3 (A). The

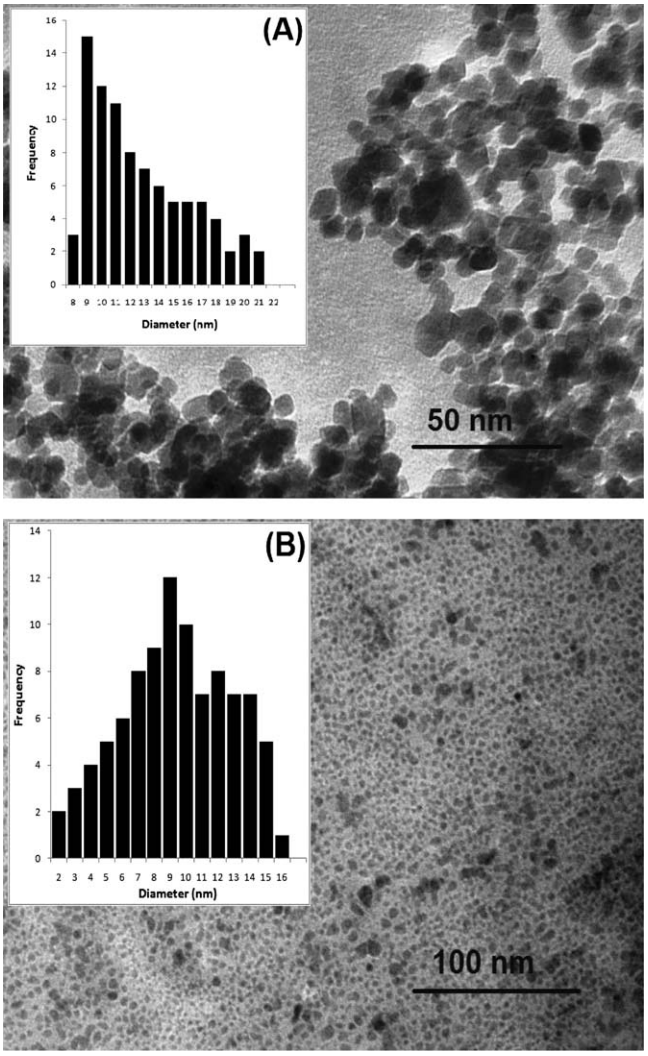

Fig. 3. TEM images of (A) pristine magnetite nanoparticles (M1); (B) magnetite nanoparticles modified with 0.5 M trisodium citrate dihydrate (CM1). The magnification of both samples are 100,000× and 60,000×, respectively.

agglomeration could probably be due to the substantial built-up specific surface area of the nano-sized particles [27]. Hu et al., however, proposed that the magnetic nanoparticles aggregated together to reduce their surface energy [28]. Besides, the particles agglomeration may also be due to the magnetic dipole–dipole interactions and the van der Waals forces between the nanoparticles [29,30]. Hence, it is our goal to modify the surface of the M1 nanoparticles with polyanionic citrate using chemisorption complexation process. Introduction of citrate group onto the surface of magnetite nanoparticles will enhance the dispersion stability of particles from the highly negatively charged citrate ions. The highly negatively charged citrate ions contribute to electrostatic repulsion between the particles when they are chemically adsorbed on the particles surface and thus increased the dispersibility of CM1. The concentrated citrate ions will be easily dissolved at high temperature (80 °C) when it is added into reaction mixture (M1 plus DIW). The water molecules in the reaction mixture causing the dissolvation of citrate salt, leading to more citrate ions formed in the solution. The negatively charged citrate ions then underwent hydrogen bonding between (–OH) hydroxyl group that are fully covered on the magnetite surfaces and the carboxyl group (–COOH) from the citrate ions. From Fig. 3 (B), it can be conjectured that almost all particles were well-modified with citrate ions in comparison with the unmodified sample (M1) because the signs of agglomeration of the particles could not be observed in the micrograph of sample CM1. Fig. 4 illustrates the citrate-modified magnetic nanoparticles (CM1) treatment process prior to the silica coating process to produce randomized dispersion magnetite nanoclusters coated with silica.

3.2. Morphological studies of different reaction parameters of silica coated magnetite nanoclusters

3.2.1. Effect of different alcohol

In this section, we employed Stöber process to coat CM1 nanoparticles with some minor modifications in order to produce randomized dispersion magnetite nanoclusters coated with silica. Stöber process was first proposed in 1968 by Werner Stöber and co-workers to prepare amorphous silica [25]. Since then frequently studies have been carried out to investigate the preparation of silica microspheres, gelling properties, morphological properties and some other mechanism studies related to the formation of the silica particles [31–34]. Essentially, this method is based on the use of precursor TEOS which is to be mixed well in the alcohol–water solution under an alkaline condition at room temperature. Tetraethyl orthosilicate (TEOS) is the source of silica and water is the medium to hydrolyze the TEOS monomer to initiate the polymerization process. The alcohol, on the other hand, is a co-solvent that is miscible with TEOS and water to provide them into the same phase enabling them to react. Ammonia is an alkaline catalyst that helps to accelerate the polymerization of TEOS to form silica. Therefore, it is our concern in the present study to endow this process to prepare randomized dispersion magnetite nanoclusters coated with silica. We investigated the effect of polarity of alcohol on the morphology of silica coated onto CM1 nanoparticles. The samples were denoted as SCM1, SCM2, SCM3, and SCM4, as shown in Fig. 5 (A–D) with respect to the use of methanol, ethanol, isopropyl alcohol, and tertiary butyl alcohol, accordingly. The amount of the reactants was fixed with some references from the literature [22,23], namely, 2 ml CM1 dispersed ferrofluid, 2 ml of TEOS, 70% v/v of alcohol–water and 2 ml of ammonia. Fig. 5 (A–D) shows the TEM images of the silica coated CM1 nanoparticles with the use of decreasing order of alcohol polarity. As can be observed from Fig. 5 (A), a large number of silica nanoparticles, with almost the same size (∼10 nm), were found in the sample SCM1 leaving a large amount of uncoated magnetite nanoparticles. As compared to Fig. 5 (B), intriguingly, the SCM2 particles were coated in such a way that the magnetite nanoparticles were well engulfed and dispersed with silica coating. There is a common similarity in the structure of randomized dispersion nanoclusters that can be seen in this sample as well. On the other hand, Fig. 5 (C) depicts that the

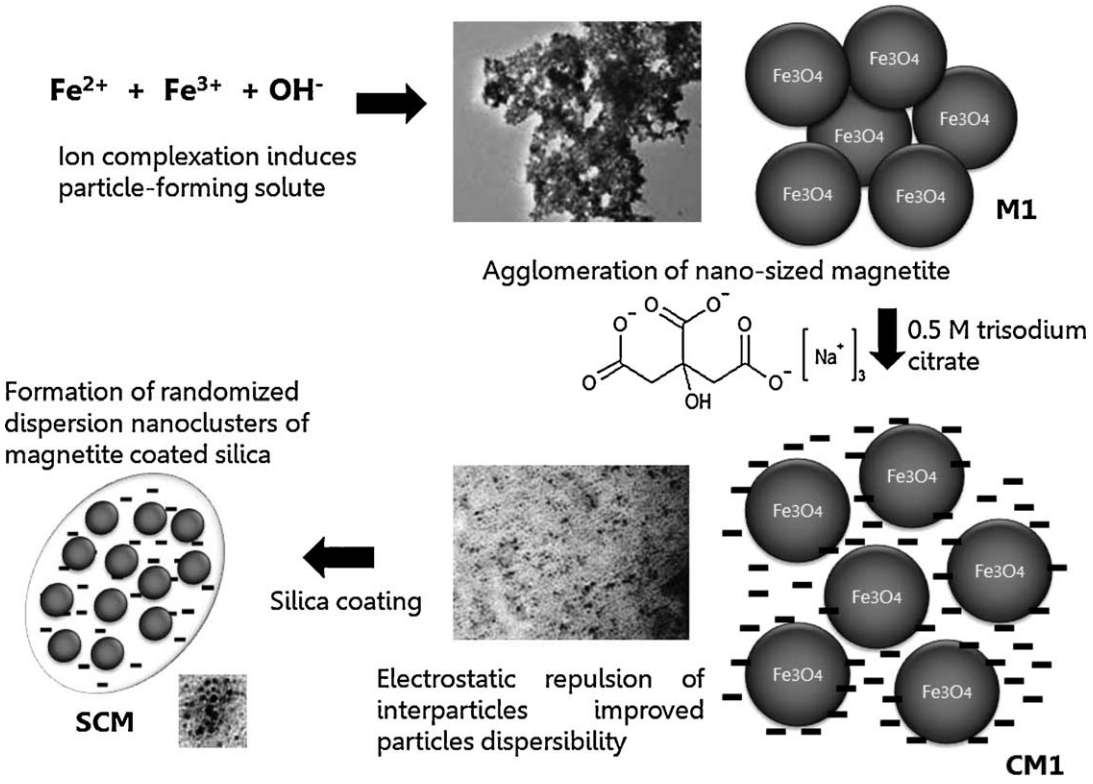

Fig. 4. Illustration of polyanionic citrate-modified magnetite nanoparticles and the formation of randomized dispersion nanoclusters of magnetite coated silica.

SCM3 particles were also coated with silica layer but rather in the irregular form. Fig. 5 (D), however, shows the SCM4 particles that appeared in the silica regime also had irregular form of coating as a result of the use of tertiary butyl alcohol as co-solvent in the TEOS polymerization. All these could be explained in terms of the polarity of the alcohol used. The polarity of alcohol is the difference of electronegativity between the partially positively charged carbon chain and the partially negatively charged hydroxyl (–OH) group. In this study, we have used methanol, ethanol, isopropyl alcohol, and tertiary butyl alcohol with decreasing polarity. Methanol has the strongest polarity due to the polar molecule (–OH) that dominates the CH short chain. Wang et al. reported that the strong polarity of methanol provides better dispersibility of magnetite nanoparticles in methanol–water solution and leads to better morphology of silica coated magnetite nanoparticles [35]. However, in our study as shown in Fig. 5 (A), majority of the products synthesized are solely silica particles in regular oval shape. This can be attributed to the strong polarity of methanol that renders rapid hydrolysis and condensation of TEOS monomer before the silica sol is chemically bond on the surface of magnetite nanoparticles. By referring to Fig. 5 (B–D), the use of alcohol with decreasing polarity has led to the adverse formation of silica coated magnetite nanoclusters due to the dominance non-polar properties of CH bond as alternated from ethanol to tertiary butyl alcohol. Apart from the changes in shape, the average size of the silica coated magnetite nanoclusters is also increased to 20 nm, 54 nm and 78 nm of SCM2 in Fig. 5 (B), SCM3 in Fig. 5 (C) and SCM4 in Fig. 5 (D), respectively. The shape of the silica coated nanoclusters also varies from nearly spherical to the cluster form. Hence, ethanol could be served as the best candidate as co-solvent in the reaction media due to its polarity that can render the formation of randomized dispersion magnetic silica clusters as compared to the other alcohols. As a result, ethanol has been chosen as a co-solvent of TEOS polymerization in the following studies.

3.2.2. *Effect of alcohol–water ratio (% v/v)*

Apart from the influence of different polarities of alcohol on the formation of different morphology of silica coated magnetite nanoclusters, the effect of ratio of ethanol–water (% v/v) has also been investigated. In this section we have manipulated the concentration of ethanol–water in total of 100 ml. Fig. 6 shows the TEM micrographs of the samples SCM-a, SCM-b, SCM-c, and SCM-d at different concentration of ethanol–water, i.e., 100% v/v, 50% v/v, 30% v/v, and 0% v/v, respectively. TEM images illustrated in Fig. 6 suggest that the greater the ratio of ethanol–water, the poorer the formation of randomized dispersion magnetic silica nanoclusters. Fig. 6 (A) shows that the sample SCM-a (100% v/v) has no rigid pattern of silica coated magnetite nanoparticles. Supposedly the scarcity of water would not initiate the polymerization of TEOS monomer, but it turned out to be that, there is sizable coverage of magnetite nanoparticles entrapped inside silica coating layer. This could be explained by the purity assay of ethanol used in the experiment, we used 95% v/v assay of ethanol instead of absolute ethanol. Therefore, the low percentage of water that remained in the reaction system

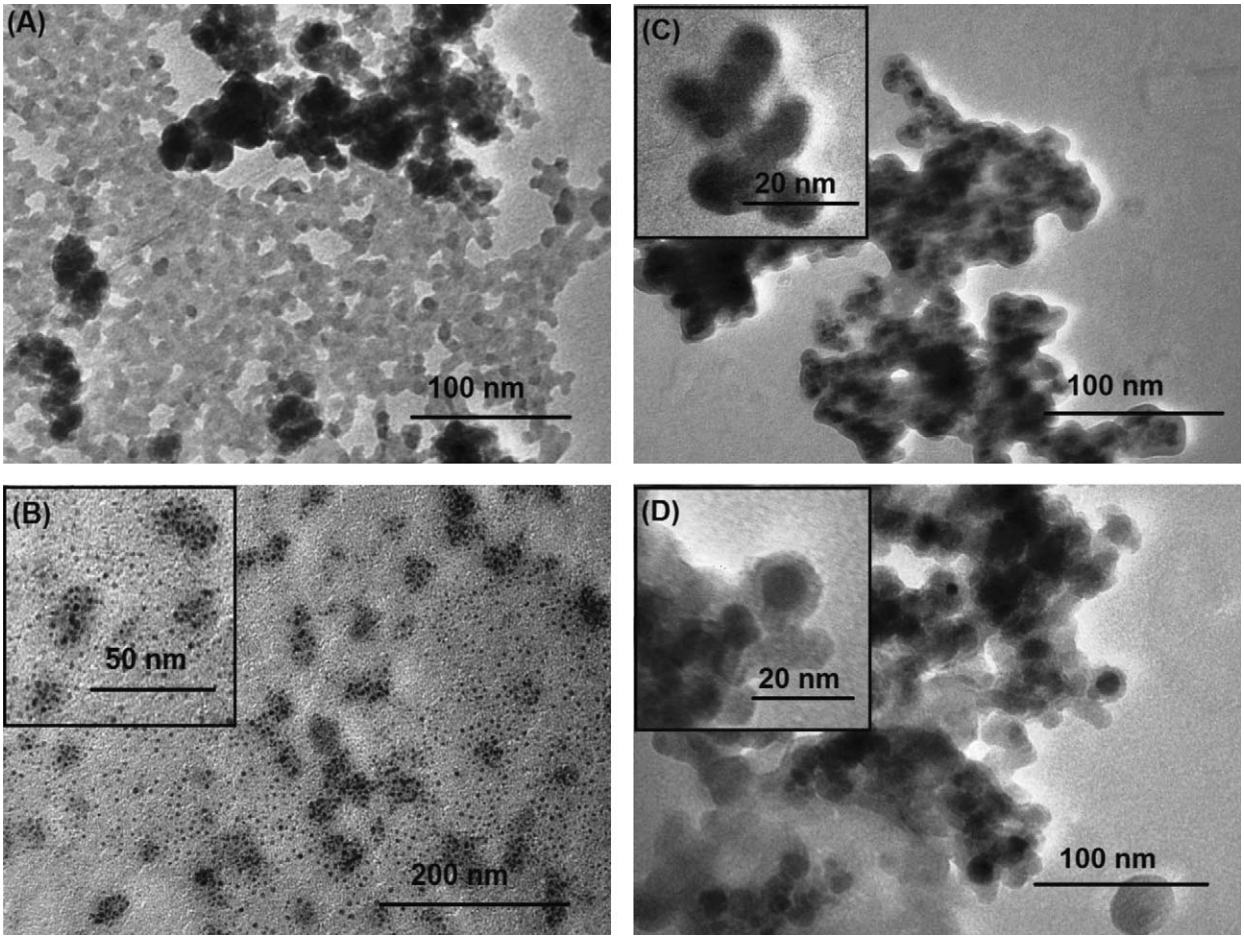

Fig. 5. TEM images of silica coated CM1 nanoparticles with different polarity of alcohol as co-solvent in the reaction system of TEOS; (A) methanol (SCM1), (B) ethanol (SCM2), (C) isopropyl alcohol (SCM3), and (D) tertiary butyl alcohol (SCM4).

presented in the ethanol would probably contribute to the occurrence of the monomer polymerization. Fig. 6 (B and C), however, depicts a significant improvement in spherical shape of silica coated magnetite nanoclusters when the percentage volume of water increased from 50 to 30% v/v. The morphologies of both samples reveal that spherical shape of the silica coated magnetite nanoclusters was favorably to be formed when the amount of water in the reaction system is increased. This is consistent with the findings of Bogush et al., that reports that when higher amount of water is used in the silica preparation process, larger silica spheres with irregular shape will be produced [36]. Fig. 6 (D) shows that the shape of the silica coated magnetite nanoclusters was massively enlarged when water (100%) was fully supplied in the reaction system. It should also be noted that there are some free magnetite particles which were not coated with silica as circled in Fig. 6 (D). This is due to the phase separation that occurred within the system since the concentration of co-solvent (ethanol in this case) is extremely low, causing TEOS monomer to be hydrolyzed and condensed entirely by water. Enomoto et al. also suggested that the ultrasonic irradiation could accelerate the hydrolysis and condensation of TEOS in the silica coated magnetite nanoclusters [37]. The results suggested that high concentration of ethanol or high amount of water is not favorable for the production of silica coated magnetite nanoclusters with well-defined structures and morphologies. Hence, we might conclude that the concentration of alcohol–water should be in the range of 70–30% v/v.

3.2.3. *Effect of alkaline catalyst (NH_3)*

In this section, different concentrations of NH_3 were added into the reaction system to accelerate the polymerization of TEOS monomer. Different volumes of NH_3, i.e., 0.5, 1, and 3 ml, were added into three batch experiments containing the same reactant parameters, i.e., 2 ml of TEOS, 70% v/v of ethanol–water, and 2 ml as-produced CM1 ferrofluid. The pH of the mixture after the addition of NH_3 (0.5, 1, and 3 ml) was recorded as 9, 11.5, 12.5, respectively, and the samples are assigned as SCM-Am0.5, SCM-Am1, and SCM-Am3. According to the TEM images depicted in Fig. 7 (A), large amount of cellulosic-like network structures was found surrounding the magnetite nanoparticles (shown in arrows). We conjectured that the network structure has started to form as a result of the initial stage of TEOS polymerizations. The silica particles could not be able to form completely due to insufficient amount of NH_3 added into the reaction system. Stöber et al. suggested that NH_3 is used as morphological catalyst to produce spherical silica particles [25]. They also reported that in the absence of NH_3,

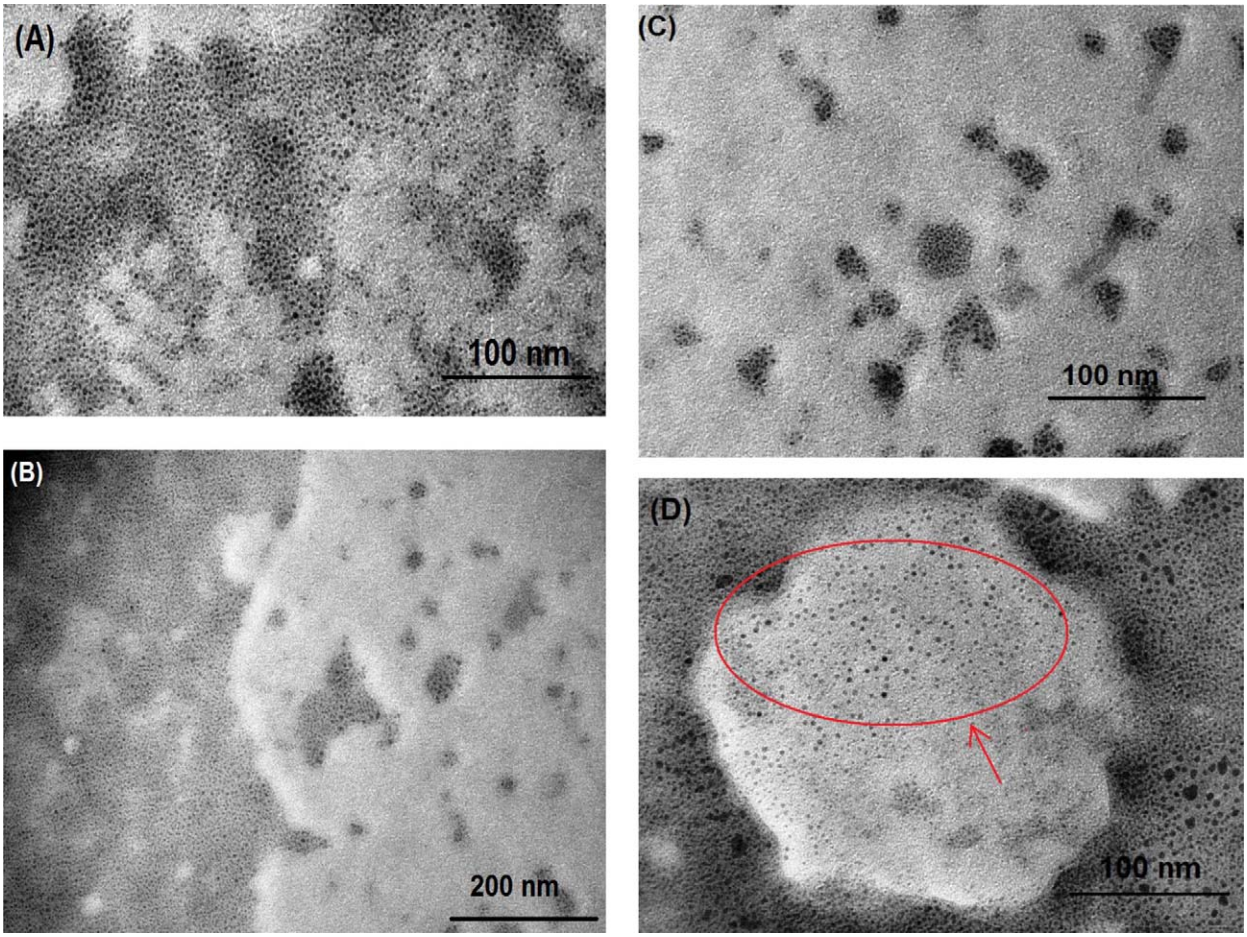

Fig. 6. TEM images of CM1 coated nanoparticles with different ratio of ethanol–water; (A) 100% v/v (SCM-a), (B) 50% v/v (SCM-b), (C) 30% v/v (SCM-c), and (D) 0% v/v (SCM-d).

silica particles flocculated to form irregular shaped aggregates. Fig. 7 (B and C) presents the TEM images of the silica coated magnetite nanoparticle samples produced by using 1 ml and 3 ml of NH_3, respectively. As the volume of NH_3 increased from 0.5 ml to 1 ml, one can see that the silica layers started to form on the surface of the magnetite nanoparticles but the rigid structures of silica coated magnetite nanoclusters still cannot be observed (Fig. 7 (B)). When the amount of NH_3 increased to 2 ml, thin layers of silica formed on the surface of magnetite nanoparticles leading to the formation of magnetite nanoparticles in nanocluster form (Fig. 5 (B)). TEM image in Fig. 7 (C) indicates that the silica coated magnetite nanoclusters formed when the amount of ammonia catalyst was increased to 3 ml. Most of the magnetite nanoparticles were successfully entrapped inside the silica sphere-like clusters. Besides, we also found that there were some silica particles simultaneously present in Fig. 7 (C) together with the silica-magnetite nanocomposites. This happened when the pH of reaction solution is high enough to induce TEOS polymerization during the addition of NH_3 and thus the excessive NH_3 accelerates the hydrolysis and condensation of TEOS, therefore blank silica particles could be observed in the SCM-Am3 [38]. From these results, we surmised that the hydrolysis and condensation rates of TEOS monomer on the surface of magnetite nanoparticles were strongly governed by the amount of NH_3 added into the reaction mixture. Hence, 2 ml of NH_3 has been used for further experiments.

3.2.4. *Effect of monomer TEOS*

We also studied the morphological properties of the silica coated magnetite nanoparticles by varying the concentration of TEOS that is added into the reaction mixture prior to the polymerization process. The other recipes of reaction were kept constant as outlined in Table 1. Zhu et al. reported that the addition of TEOS significantly affects the thickness of the silica layer [39]. In Fig. 8 (A), one can see that the CM1 particles were well-coated with a silica layer. The thickness of the silica layer was measured in the range of 10.8–12.6 nm as shown in Fig. 8 (A). As the volume of TEOS was increased to 4 ml, apparently the layer of the silica coating (Fig. 8 (B)) was much thicker than that of the previous one in Fig. 8 (A). We have measured the size of the silica coated magnetite nanoclusters with the use of TEM micrographic processing software and eventually it cannot be done since the nanoclusters appeared in the aggregated form. However, the silica thickness layer can be measured and the value of the layers was determined in the range from 27.3 nm to 35.8 nm which has been shown in Fig. 8 (B). The thickness of the silica layer for both SCM-T3 and

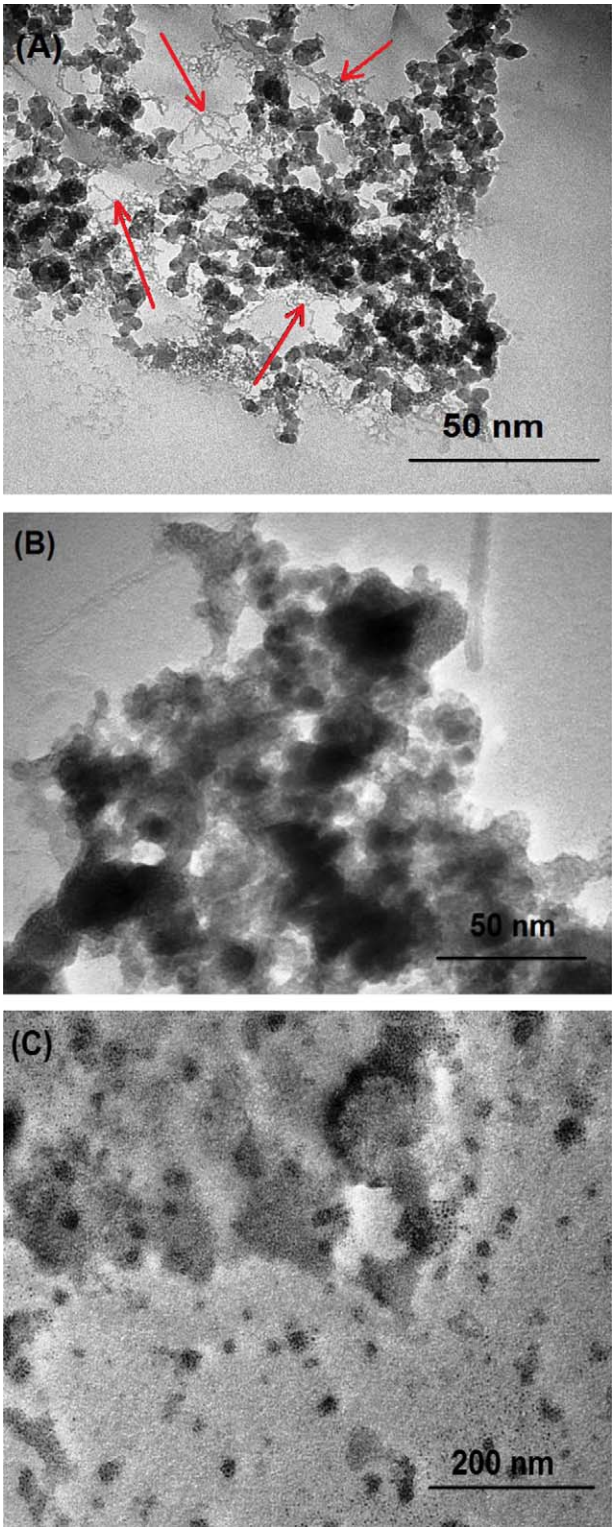

Fig. 7. TEM images of silica coated CM1 nanoparticles with different amounts of ammonia (NH_3) added into the reaction system; (A) 0.5 ml (SCM-Am0.5), (B) 1 ml (SCM-Am1), and (C) 3 ml (SCM-Am3).

SCM-T4 samples appeared in irregular nanoclusters shape when compared to that of the sample SCM2 (Fig. 5 (B)). It is found that the nanomaterials in sample SCM2 were much better in shape and possess well-defined nanoclusters structure although the silica coating layer for SCM2 was much thinner

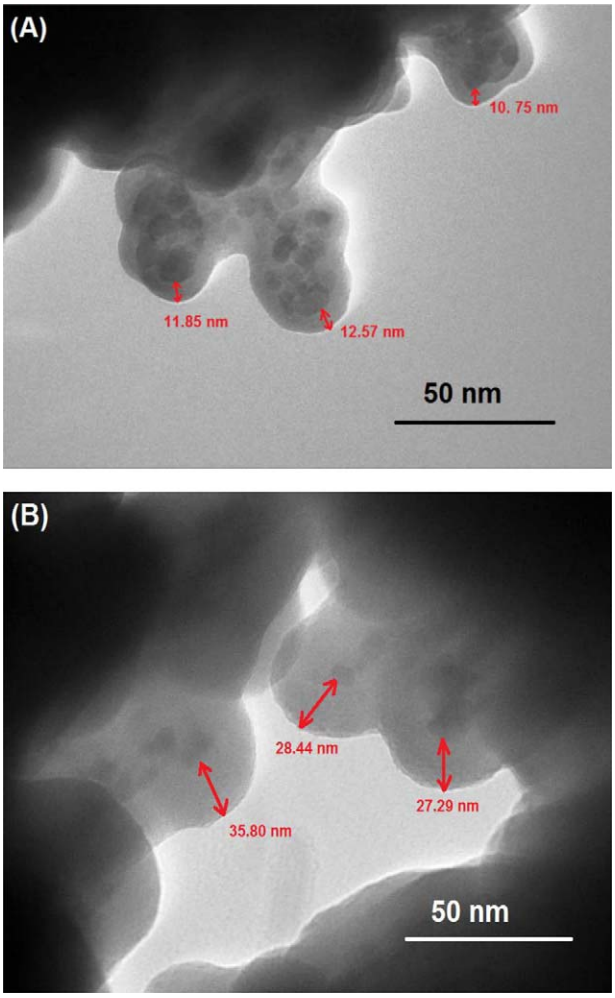

Fig. 8. TEM images of silica coated CM1 nanoparticles with varying amounts of TEOS monomer; (A) 3 ml of TEOS (SCM-T3) and (B) 4 ml of TEOS (SCM-T4).

than that of the SCM-T3 and SCM-T4. Previous study suggested that the higher the amount of TEOS monomer presented in the reaction system, the more the irregular shape of nanoclusters composite will be formed due to rapid polymerization of TEOS in excessive amount [40].

3.3. X-ray diffraction (XRD)

The degree of crystallinity of the prepared magnetic samples was examined by XRD Bruker D-8 advance spectra. Fig. 9 shows the XRD spectra of three samples SCM2, CM1, and M1, respectively, in comparison to the characteristic peaks of the standard JCPDS pattern (00-019-0629). The characteristic peaks in the spectra are corresponding to the $d_{h\,k\,l}$ crystal planes of magnetite (2 2 0), (3 1 1), (2 2 2), (4 0 0), (4 2 2), (5 1 1) and (4 4 0). It can be seen that all the characteristic peaks of the three samples are well-coincided with respect to the standard peaks. There is no other undesired diffraction maximums of the impurities that can be observed from the spectra and the as-produced magnetite samples are found to exist in inverse cubic spinel structure [41]. Interestingly, it is noted that the spectrum

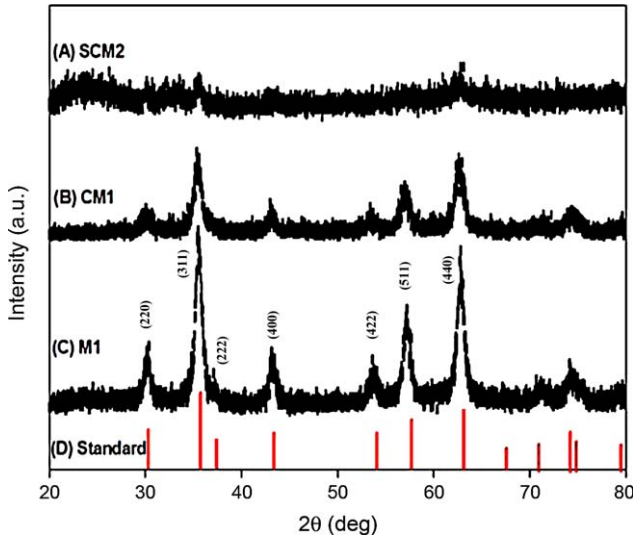

Fig. 9. XRD spectra of (A) silica coated magnetite nanoclusters (denoted as SCM2), (B) citrate-modified nanoparticles (denoted as CM1), (C) pristine nanoparticles (denoted as M1), and (D) standard peak of magnetite crystallite provided by JCPDS: 19-0629.

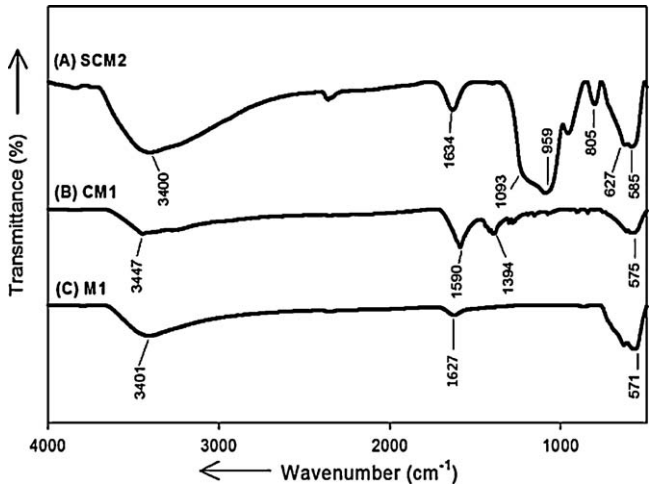

Fig. 10. FT-IR spectra of the (A) silica coated nanoclusters (SCM2), (B) citrate-modified nanoparticles (CM1), and (C) pristine nanoparticles (M1).

for sample SCM2 (silica coated magnetic nanoclusters with pre-determined reaction parameters) consisted of amorphous structure in between the range of 20° and 30° 2θ region which is attributed to the amorphous silica matrix, as being clearly indicated in Fig. 9 (A) [42]. The relatively low intensity reflections and no significant sharp diffraction peaks for SCM2 spectrum are probably due to the presence of surface SiO_2 on the surface of magnetic nanoparticles. Xu et al. also suggested that the low intensity of reflection peaks could be attributed to the ultrafine crystalline of the magnetite particles present in the silica coated nanoclusters [43]. The XRD results indicate that the nanoclusters of magnetite coated with silica have been successfully prepared without the alteration to the crystal structure of magnetite nanoparticles and the crystallinity of the magnetite is well preserved although the nanoparticles have been modified superficially with silica and citrate ions.

3.4. FT-IR analysis

Fig. 10 depicts the FT-IR spectra of the as-synthesized silica coated magnetite nanoparticles (SCM2), citrate-modified magnetite nanoparticles (CM1), and pristine magnetite nanoparticles (M1). For the unmodified magnetite nanoparticles, there is an intense absorption band that could be observed at 571 cm^{-1} which can be attributed to the torsional vibration and stretching mode of the Fe–O bond [44]. Apart from that peak, two broad bands centred at 1627 and 3401 cm^{-1} can also be seen in the M1 spectrum due to O–H stretching mode of vibration of free or adsorbed water that still remained in the sample [45]. The absorption peak of magnetite at 575 cm^{-1} is also clearly visible in the sample CM1 as shown in Fig. 10 (B). This implies that the sample CM1 does not change chemically or physically after the treatment with trisodium citrate dihydrate. Comparably, two new absorbent peaks appearing at 1394 and 1590 cm^{-1} are due to the carboxyl group of sodium citrate. Specifically, these two peaks are attributed to the –COO– symmetric and antisymmetric stretching, respectively [46]. It suggested that the complexation between the citrate groups and Fe ions were found to occur on the surface of magnetite nanoparticles. The characteristic peak at around 3447 cm^{-1} is also visible in the spectrum of CM1 which confirms the presence of physically absorbed free water molecules on the magnetite surface after the modification with sodium citrate. Fig. 10 (A) shows the IR spectrum of silica coated magnetite nanoparticles (SCM2). Also, the absorption peak of Fe–O bond at around 585 cm^{-1} can be observed in the spectrum for SCM2. There is also a weak signal of absorbance at 627 cm^{-1} which could be attributed to the stretching vibration of Si–C bond. Furthermore, two absorption peaks centred at around 805 and 1093 cm^{-1} can also be observed, corresponding to the stretching of Si–O–Si bond from the silica particles. On the other hand, our study has shown that a low intensity of signal at 959 cm^{-1} was observed as well. This peak is referred to the Si–OH deformation as a result of incomplete condensation of TEOS sol [44]. The presence of two broad bands appearing at 1634 and 3400 cm^{-1} is an indication of the presence of free H–O–H molecules in the SCM2 sample. Apart from that it can also be attributed to hydrophilicity of the silica layer which has great ability to absorb water. All the aforementioned peaks are outlined in Table 2 with the assignments of the associated functional groups. From the above results, it can be inferred that the citrate polyanions complexes and SiO_2 have been successfully coated on the surface of magnetite nanoparticles.

3.5. VSM

The hysteresis loops for three samples (M1, CM1, and SCM2) recorded at room temperature (298 K) are depicted in Fig. 11 (A–C). As can be noticed, the saturation magnetization (M_s) of the three samples, M1, CM1, and SCM2, was 52.13, 37.45, and 0.65 emu/g, respectively. Clearly, the M_s value for M1 was expectedly lower than that of the bulk magnetite (~92 emu/g) due to their finite size [47]. The external magnetic

Table 2
FT-IR absorbance wavenumber and the assignments of the functional groups.

IR wavenumber (cm^{-1})	Assignments
571, 575 and 585	υ(Fe–O)
627	υ(SiC)
805 and 1093	υ_s(Si–O–Si)
959	δ(Si–OH)
1394	υ_s(–COO–)
1590	υ_a(–COO–)
1627 and 1634	H–O–H
3400, 3401 and 3447	H–O–H

Key: υ: stretch, υ_s: symmetrical stretch, υ_a: antisymmetrical stretch, δ: deformation.

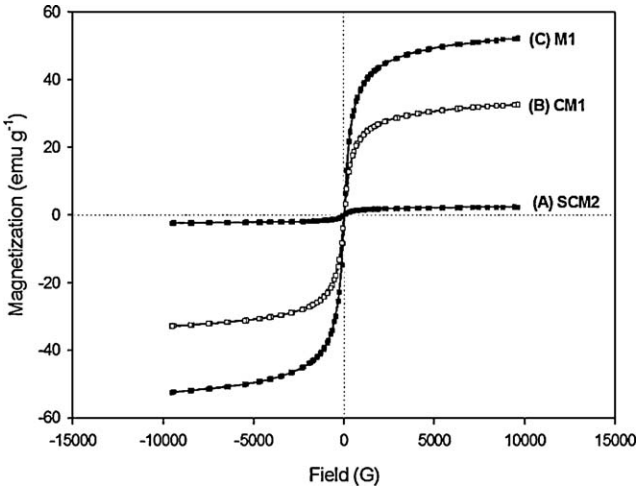

Fig. 11. Variation of magnetization values with the applied field at 298 K for; (A) silica coated magnetite nanoclusters (SCM2), (B) citrate-modified magnetite nanoparticles (CM1), and (C) pristine magnetite nanoparticles (M1).

field is proportional to the particle size via the number of magnetic molecules in a single-domain. This phenomenon is rather significant for the nano-sized particles due to their large surface area to volume ratio. The lower M_s value for both the surface-modified magnetite nanoparticles (CM1 and SCM2) could be explained by the presence of non-magnetic layer on the particles surface. The diamagnetic layer of the citrate anions and silica coating on the surface of magnetite nanoparticles weakened the magnetic moment of the inner core magnetic nanoparticles [48].

In addition, the three samples (M1, CM1, and SCM2) exhibited nearly zero remanence and coercivity as demonstrated in Fig. 11 (A–C). This affirmatively proved that the samples possess superparamagnetic behaviour. Taking into consideration that the coercivity of the particles is governed by the domain wall movement, the relatively small coercivity displayed by our samples especially sample SCM2, i.e., the randomized dispersion magnetite nanoclusters coated with silica, indicated that the magnetite nanoclusters assembled is magnetized in same direction by applied field. The particles are easily magnetized along with the applied field and will randomize dispersed to lose their magnetization as soon as the applied field is turned off. A sturdy evidence shown in Fig. 12 demonstrated that our silica coated magnetite nanoclusters are well-dispersed and possess superparamagnetic behaviour when dispersed in the ethanol solution. In the absence of external magnetic field, the nanoclusters are dispersed very well without any flocculation. Comparably, under the influence of external magnetic field, the nanoclusters are immediately attracted to the side of the vial where the magnet bar is placed. This demonstration implies that the sample has excellent superparamagnetic properties and could be considered for potential usage in biomedical application such as drug delivery, and MRI contrast.

3.6. TGA

Typical TG weight loss versus temperature curves for the samples M1, CM1 and SCM2 are illustrated in Fig. 13. As one can be referred to Fig. 13 (C), no significant weight loss below 100 °C could be observed for M1 sample and only a small change in mass percentage could be seen in the temperature

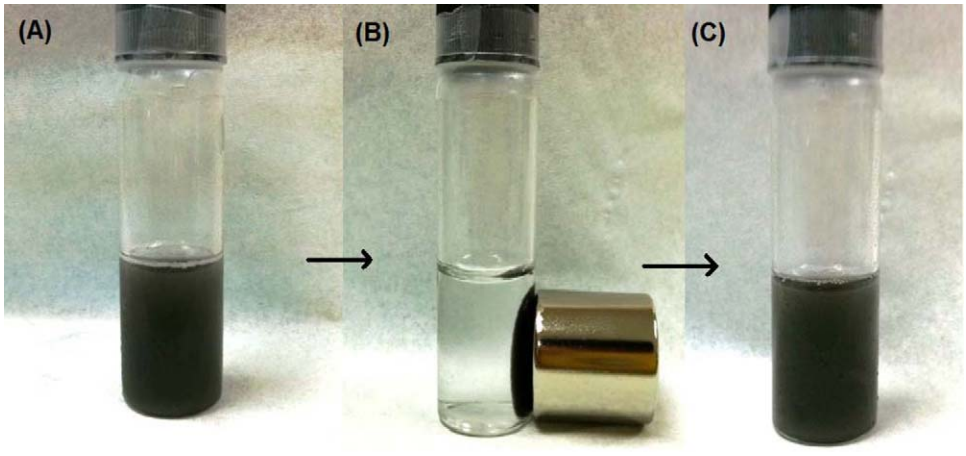

Fig. 12. The as-synthesized silica coated magnetite nanoclusters dissolved in ethanol solution; (A) well dispersed without the presence of external magnetic field, (B) the particles immediately collected to the wall of sample vial upon the placement of a magnet, and (C) the particles re-dispersed into the solution by gentle shaking after the removal of the magnet.

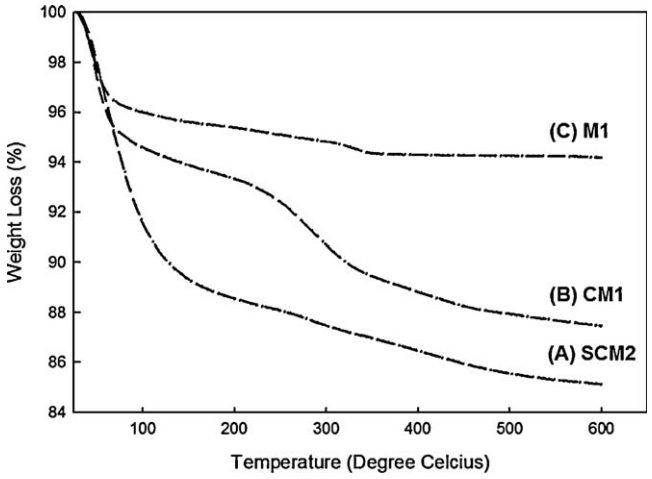

Fig. 13. Thermogravimetric (TG) curves for (A) silica coated magnetite nanoclusters (SCM2), (B) citrate-treated magnetite nanoparticles (CM1), and (C) pristine magnetite nanoparticles (M1).

range of 100–250 °C. The weight loss recorded as 1.84 wt.% in this temperature range mainly resulted from the release of water molecules bonded physically and chemically in the magnetite nanoparticles [9]. The TG curve of the citrate-treated magnetite nanoparticles (CM1) which was represented by Fig. 13 (B), however, shows three separate stages that occurred at around 100, 260, and 430 °C. The first weight loss at ∼100 °C is due to the loss of water (3.14 wt.%). The major weight loss of 2.97 wt.% (of the original mass) at ∼260 °C and 1.07 wt.% at ∼430 °C is attributed to the decomposition of citrate group which is chemically bonded onto the surface of magnetite nanoparticles [46]. For the silica coated magnetite nanoclusters (SCM2) which was depicted in Fig. 13 (A), show significant weight loss when exposed to high temperature. The total silica and citrate content of SCM2 was estimated to be 9.26 wt.%. Although the trend of weight loss was not steadily same between the SCM2 and CM1, the total percentage of weight loss for the former is found to be higher. This further confirmed the presence of citrate group and amorphous silica in the SCM2. A remarkable drop in weight at ∼120 °C for the SCM2 sample has proven its high affinity in water absorption due to the hydrophilicity behaviour of the amorphous silica [49].

4. Conclusion

In summary, herein we report a way to study the morphology of randomized dispersion magnetite nanoclusters coated with silica by controlling several reaction parameters during the silica sol polymerization process. The magnetite nanoparticles were firstly prepared using a well-known method i.e., co-precipitation, followed by surface-modification with poly-anionic trisodium citrate dihydrate. The citrate-treated magnetite nanoparticles were then coated with silica using Stöber method with some minor modifications. Effects of alcohols with different polarities as co-solvents, ratio of alcohol–water, amount of NH_3 as a catalyst and amount of TEOS monomer were elucidated on the formation of nanoclusters. Examinations using TEM, XRD, FT-IR, VSM, and TGA were carried out to characterize the pristine magnetite nanoparticles, citrate-modified, and silica coated magnetite nanoclusters. The results revealed that before the modification with citrate group, comparatively, the modified magnetite nanoparticles showed an enhancement in particles dispersibility and better size distribution. In addition, the best ratio of alcohol–water was confirmed to be within 70–30% v/v to produce well defined and randomized dispersion magnetite nanoclusters. Further investigations on the formation of magnetite nanoclusters using alcohols with different polarities show that ethanol is preferable in the formation of nanoclusters due to its moderate polarity rendering the formation of nanoclusters with desired shape and randomize dispersivity. We also studied the effect of NH_3 as alkaline catalyst on the formation of silica coated magnetite nanoclusters. TEM results demonstrated that the amount of NH_3 should be well determined since it might induce the formation of blank silica particles before it is able to be coated on the magnetite nanoparticles surface. Apart from that, the concentration of TEOS monomer also plays a crucial role in the formation of magnetite nanoclusters. The TEM results indicated that the thickness of the silica layer on the surface of magnetite nanoparticles is increased with the amount of TEOS that has been utilized during the synthetic process, even after the silica coating process. XRD analysis has proven that the as-synthesized magnetites retained the good crystalline characteristics. The presence of the silica coating and citrate group on the magnetite nanoparticles has been attested from the FT-IR absorbance peaks. We also confirmed the superparamagnetic behaviour of the as-synthesized products by using VSM at room temperature. TG analysis has proven the structure and composition of the citrate-treated and silica coated magnetite nanoclusters. Further works on the applications of the silica-coated magnetite nanoclusters in drug delivery are underway in order to validate their potential usage in high efficiency targeted drug delivery system, especially for cancer treatment application.

Acknowledgement

This project was supported by Universiti Kebangsaan Malaysia under the Research University Operation Grants (UKM-OUP-NBT-28-124/2010 & UKM-OUP-NBT-29-142/2010) and the Young Researcher Grant (UKM-GGPM-NBT-085-2010). Haw acknowledges the Ministry of Science, Technology and Innovation (MOSTI) for the disbursement of National Science Fellowship (NSF).

References

[1] C. Barrera, A. Herrera, Y. Zayas, S. Rinaldi, Surface modification of magnetite nanoparticles for biomedical applications, Journal of Magnetism and Magnetic Materials 321 (10) (2009) 1397–1399.

[2] J. Zhi, Y. Wang, Y. Lua, J. Maa, G. Luo, In situ preparation of magnetic chitosan/Fe_3O_4 composite nanoparticles in tiny pools of water-in-oil microemulsion, Reactive and Functional Polymers 66 (12) (2006) 1552–1558.

[3] S. Xuan, L. Hao, W. Jiang, X. Gong, Y. Hua, Z. Chen, Preparation of water-soluble magnetite nanocrystals through hydrothermal approach, Journal of Magnetism and Magnetic Materials 308 (2) (2007) 210–213.
[4] S. Chaianansutcharit, O. Mekasuwandumrong, P. Praserthdam, Synthesis of Fe_2O_3 nanoparticles in different reaction media, Ceramics International 33 (4) (2007) 697–699.
[5] I. Nedkova, T. Merodiiskaa, L. Slavova, R.E. Vandenbergheb, Y. Kusanoc, J. Takada, Surface oxidation, size and shape of nano-sized magnetite obtained by co-precipitation, Journal of Magnetism and Magnetic Materials 300 (2) (2006) 358–367.
[6] C.C. Hua, S. Zakaria, R. Farahiyan, T.K. Liew, K.L. Nguyen, M. Abdullah, S. Ahmad, Size-controlled synthesis and characterization of Fe_3O_4 nanoparticles by chemical coprecipitation method, Sains Malaysiana 37 (4) (2008) 389–394.
[7] M. Ma, Y. Zhang, W. Yu, H. Shen, H. Zhang, N. Gu, Preparation and characterization of magnetite nanoparticles coated by amino silane, Colloids and Surfaces A: Physicochemical and Engineering Aspects 212 (2–3) (2003) 219–226.
[8] S. Chairam, E. Somsook, Starch vermicelli template for synthesis of magnetic iron oxide nanoclusters, Journal of Magnetism and Magnetic Materials 320 (15) (2008) 2039–2043.
[9] S. Purushotham, R.V. Ramanujan, Thermoresponsive magnetic composite nanomaterials for multimodal cancer therapy, Acta Biomaterialia 6 (2) (2010) 502–510.
[10] A.Z.M. Badruddoza, K. Hidajat, M.S. Uddin, Synthesis and characterization of [β]-cyclodextrin-conjugated magnetic nanoparticles and their uses as solid-phase artificial chaperones in refolding of carbonic anhydrase bovine, Journal of Colloid and Interface Science 346 (2) (2010) 337–346.
[11] L. Zhang, X. Zhu, H. Sun, G. Chi, J. Xu, Y. Sun, Control synthesis of magnetic Fe_3O_4-chitosan nanoparticles under UV irradiation in aqueous system, Current Applied Physics 10 (3) (2010) 828–833.
[12] C.P. Chen, T.H. Chang, T.F. Wang, Synthesis of magnetic nano-composite particles, Ceramics International 28 (8) (2002) 925–930.
[13] E. Duguet, S. Vasseur, S. Mornet, G. Goglio, A. Demourgues, J. Portier, F. Grasset, P. Veverka, E. Pollert, Towards a versatile platform based on magnetic nanoparticles for in vivo applications, Bulletin of Materials Science 29 (6) (2006) 581–586.
[14] S. Guo, D. Li, L. Zhang, J. Lia, E. Wang, Monodisperse mesoporous superparamagnetic single-crystal magnetite nanoparticles for drug delivery, Biomaterials 30 (10) (2009) 1881–1889.
[15] F.C. Meldrum, N.A. Kotov, J.H. Fendler, Preparation of particulate mono- and multilayers from surfactant-stabilized, nanosized magnetite crystallites, Journal of Physical Chemistry 98 (17) (1994) 4506–4510.
[16] Z. Huang, F. Tang, Preparation, structure, and magnetic properties of polystyrene coated by Fe_3O_4 nanoparticles, Journal of Colloid and Interface Science 275 (1) (2004) 142–147.
[17] J. Liu, Y. Deng, C. Liu, Z. Sun, D. Zhao, A simple approach to the synthesis of hollow microspheres with magnetite/silica hybrid walls, Journal of Colloid and Interface Science 333 (1) (2009) 329–334.
[18] J. Ugelstad, L. Söderberg, A. Berge, J. Bergström, Monodisperse polymer particles – a step forward for chromatography, Nature 303 (1983) 95–96.
[19] Y. Sun, B. Wang, H. Wang, J. Jiang, Controllable preparation of magnetic polymer microspheres with different morphologies by miniemulsion polymerization, Journal of Colloid and Interface Science 308 (2) (2007) 332–336.
[20] D.M. Souza, A.L. Andrade, J.D. Fabris, P. Valério, A.M. Góes, M.F. Leite, R.Z. Domingues, Synthesis and in vitro evaluation of toxicity of silica-coated magnetite nanoparticles, Journal of Non-Crystalline Solids 354 (42–44) (2008) 4894–4897.
[21] R.V. Ferreira, I.L.S. Pereira, L.C.D. Cavalcante, L.F. Gamarra, S.M. Carneiro, E. Amaro Jr., J.D. Fabris, R.Z. Domingues, A.L. Andrade, Synthesis and characterization of silica-coated nanoparticles of magnetite, Hyperfine Interactions 195 (1–3) (2010) 265–274.
[22] T. Sen, I.J. Bruce, Mesoporous silica–magnetite nanocomposites: fabrication, characterisation and applications in biosciences, Microporous and Mesoporous Materials 120 (3) (2009) 246–251.
[23] L.L. Qu, S.L. Tie, Mesoporous silica-coated superparamagnetic magnetite functionalized with CuO and its application as a desulfurizer, Microporous and Mesoporous Materials 117 (1–2) (2009) 402–405.
[24] K.S. Chou, C.C. Chen, The critical conditions for secondary nucleation of silica colloids in a batch Stöber growth process, Ceramics International 34 (7) (2008) 1623–1627.
[25] W. Stöber, A. Fink, E. Bohn, Controlled growth of monodisperse silica spheres in the micron size range, Journal of Colloid and Interface Science 26 (1) (1968) 62–69.
[26] P.S. Haddad, E.L. Duarte, M.S. Baptista, G.F. Goya, C.A.P. Leite, R. Itri, Synthesis and characterization of silica-coated magnetic nanoparticles, Surface and Colloid Science 128 (2004) 232–238.
[27] D.H. Chen, X.R. He, Synthesis of nickel ferrite nanoparticles by sol–gel method, Materials Research Bulletin 36 (7–8) (2001) 1369–1377.
[28] C. Hu, Z. Gao, X. Yang, Fabrication and magnetic properties of Fe_3O_4 octahedra, Chemical Physics Letters 429 (4–6) (2006) 513–517.
[29] Y. Lalatonne, J. Richardi, M.P. Pileni, Van der Waals versus dipolar forces controlling mesoscopic organizations of magnetic nanocrystals, Nature Materials 3 (2) (2004) 121–125.
[30] P.A. Hartley, G.D. Parfitt, L.B. Pollack, The role of the van der Waals force in the agglomeration of powders containing submicron particles, Powder Technology 42 (1) (1985) 35–46.
[31] Q. Huo, J. Feng, F. Schüth, G.D. Stucky, Preparation of hard mesoporous silica spheres, Chemistry of Materials 9 (1) (1997) 14–17.
[32] T. Jesionowski, J. Zurawska, A. Krysztafkiewicz, M. Pokora, D. Waszak, W. Tylus, Physicochemical and morphological properties of hydrated silicas precipitated following alkoxysilane surface modification, Applied Surface Science 205 (1–4) (2003) 212–224.
[33] J. Lee, Y. Lee, J.K. Youn, H.B. Na, T. Yu, H. Kim, S.M. Lee, Y.M. Koo, J.H. Kwak, H.G. Park, H.N. Chang, M. Hwang, J.G. Park, J. Kim, T. Hyeon, Simple synthesis of functionalized superparamagnetic magnetite/silica core/shell nanoparticles and their application as magnetically separable high-performance biocatalysts, Biocompatible Materials 4 (1) (2008) 143–152.
[34] M. Yamane, S. Aso, T. Sakaino, Preparation of a gel from metal alkoxide and its properties as a precursor of oxide glass, Journal of Materials Science 13 (4) (1978) 865–870.
[35] H. Wang, H. Nakamura, K. Yao, H. Maeda, E. Abe, Effect of solvents on the preparation of silica-coated magnetic particles, Chemistry Letters 30 (11) (2001) 1168–1169.
[36] G.H. Bogush, M.A. Tracy, C.F. Zukoski IV, Preparation of monodisperse silica particles: control of size and mass fraction, Journal of Non-Crystalline Solids 104 (1) (1988) 95–106.
[37] N. Enomoto, S. Maruyama, Z. Nakagawa, Agglomeration of silica spheres under ultrasonication, Journal of Material Research 12 (1997) 1410–1415.
[38] T. Matsoukas, E. Gulari, Monomer-addition growth with a slow initiation step: a growth model for silica particles from alkoxides, Journal of Colloid and Interface Science 132 (1) (1989) 13–21.
[39] M. Zhu, G. Qian, Z. Wang, M. Wang, Fabrication of nanoscaled silica layer on the surfaces of submicron SiO_2–Ag core–shell spheres, Materials Chemistry and Physics 100 (2–3) (2006) 333–336.
[40] C. Vogt, M.S. Toprak, M. Muhammed, S. Laurent, J.L. Bridot, R.N. Müller, High quality and tuneable silica shell–magnetic core nanoparticles, Journal of Nanoparticle Research 12 (4) (2009) 1137–1147.
[41] I. Nedkov, S. Kolev, K. Zadro, K. Krezhov, T. Merodiiska, Crystalline anisotropy and cation distribution in nanosized quasi-spherical ferroxide particles, Journal of Magnetism and Magnetic Materials 272–276 (2004) 1175–1176.
[42] H.F. Poulsen, J. Neuefeind, H.B. Neumann, J.R. Schneider, M.D. Zeidler, Amorphous silica studied by high energy X-ray diffraction, Journal of Non-Crystalline Solids 188 (1995) 63–74.
[43] H. Xu, N. Tong, L. Cui, Y. Lu, H. Gu, Preparation of hydrophilic magnetic nanospheres with high saturation magnetization, Journal of Magnetism and Magnetic Materials 311 (1) (2007) 125–130.
[44] Y.S. Li, J.S. Church, A.L. Woodhead, F. Moussa, Preparation and characterization of silica coated iron oxide magnetic nano-particles, Spectrochimica Acta Part A: Molecular and Biomolecular Spectroscopy 76 (5) (2010) 484–489.

[45] M.E. Khosroshahi, L. Ghazanfari, Preparation and characterization of silica-coated iron-oxide bionanoparticles under N_2 gas, Physica E: Low-dimensional Systems and Nanostructures 42 (6) (2010) 1824–1829.

[46] C. Cheng, Y. Wen, X. Xu, H. Gu, Tunable synthesis of carboxyl-functionalized magnetite nanocrystal clusters with uniform size, Journal of Materials Chemistry 19 (2009) 8782–8788.

[47] T. Ozkaya, M.S. Toprak, A. Bayka, H. Kavas, Y. Köseoğlu, B. Aktaş, Synthesis of Fe_3O_4 nanoparticles at 100 °C and its magnetic characterization, Journal of Alloys and Compounds 472 (1–2) (2008) 18–23.

[48] A. Mamedov, J. Ostrander, F. Aliev, N.A. Kotov, Stratified assemblies of magnetite nanoparticles and montmorillonite prepared by the layer-by-layer assembly, Langmuir 16 (8) (2000) 3941–3949.

[49] P.I. Girginova, A.L. Daniel-da-Silva, C.B. Lopes, P. Figueira, M. Otero, V.S. Amaral, E. Pereira, T. Trindade, Silica coated magnetite particles for magnetic removal of Hg^{2+} from water, Journal of Colloid and Interface Science 345 (2) (2010) 234–240.